The 2009 IEEE/RSJ International Conference on
Intelligent Robots and Systems
October 11-15, 2009 St. Louis, USA

A Visual Navigation System for Autonomous Flight of Micro Air Vehicles

Farid Kendoul and Kenzo Nonami
Robotics and Systems Control Lab, Department of Electronics and Mechanical Engineering
Chiba University, 263-8522, Chiba City, Japan

***Abstract*— Many applications of unmanned aerial vehicles (UAVs) require the capability to navigate to some goal and to perform precise and safe landing. In this paper, we present a visual navigation system as an alternative pose estimation method for environments and situations in which GPS is unavailable. The developed visual odometer is an incremental procedure that estimates the vehicle's ego-motion by extracting and tracking visual features, using an onboard camera. For more robustness and accuracy, the visual estimates are fused with measurements from an Inertial Measurement Unit (IMU) and a Pressure Sensor Altimeter (PSA) in order to provide accurate estimates of the vehicle's height, velocity and position relative to a given location. These estimates are then exploited by a nonlinear hierarchical controller for achieving various navigation tasks such as take-off, landing, hovering, target tracking, etc. In addition to the odometer description, the paper presents validation results from autonomous flights using a small quadrotor UAV.**

I. INTRODUCTION

There is a growing interest in using aerial robotic systems for inspecting and exploring dangerous and complex environments such as disaster areas, battlefields, etc. Autonomous guidance and navigation to the site of interest requires accurate estimates about the vehicle's motion. Unmanned vehicles normally rely on Global Navigation Satellite Systems (GNSS) such as GPS and GLONASS to provide position and velocity information for navigation. However, GNSS-based navigation depends on the existence of, and access to signals from satellites. Furthermore, most robotic missions are defined within the environment. Terrain Relative Navigation (TRN) is thus necessary to achieve these missions.

Terrain relative navigation can be defined as a process that consists in determining the relative position and/or relative velocity of a mobile agent (UAV, missile, planetary spacecraft, robot, etc.) with respect to a surrounding environment (terrain, target, etc). This can be done by matching *a priori* known information or pre-registered maps of the terrain with measurements obtained by the vehicle in real time using active sensors (radar, lidar, etc.) or passive imaging sensors (single camera, stereo camera, etc.). First TRN systems were developed for cruise missiles navigation such as TERrain COntour Matching (TERCOM) and Digital Scene-Mapping and Area Correlation (DSMAC) which are still used independently, or in conjunction with GNSS.

Fig. 1. A quadrotor UAV during vision-based landing on a selected target.

Recently, there is a growing interest in developing navigation systems for small UAVs operating in GPS-denied environments. Among many active sensors for environment mapping and obstacles detection, Laser Range Finder (LRF) is widely used for obstacles avoidance [1] and indoor localization [2], [3]. On the other hand, vision systems are passive and outperform active navigation systems in terms of cost, weight, power consumption and size, and are therefore excellent sensing technology for many aerial platforms and various environments. In recent years, there is an active research in developing and applying vision systems for UAVs guidance and navigation. Visual SLAM [4], [5], stereo vision [6], [7] and Structure-From-Motion [8], [9] techniques are generally used as visual navigation systems to localize and estimate the UAV ego-motion. Target relative navigation systems have been also successfully employed to land a UAV on some ground target [10] or to track an aerial target [11].

This paper describes a vision-based relative motion estimator that can be used for flight control, accurate landing and target tracking. Functionally, a vision algorithm detects and

Dr. F. Kendoul is with the Robotics and Systems Control Lab., Chiba University: fkendoul@restaff.chiba-u.jp
Professor K. Nonami is with the Robotics and Systems Control Lab., Chiba University: nonami@faculty.chiba-u.jp

tracks visual features based on monocular images obtained from an on-board single camera looking downwards. By continuously tracking ground objects that appear in the camera Field Of View (FOV) and accumulating or integrating their image displacement, it is possible to estimate the travelled flight distance in terms of total image displacement (in pixels). These visual measurements are then fused with IMU data in order to overcome the non-desired rotation effects. Indeed, it is difficult to sense UAV translation with vision alone since image displacements also occur with aircraft rotation (translation-rotation ambiguity). Another ambiguity is the scale factor or the unknown range that can not be estimated from visual measurements alone. Therefore, the vision algorithm has been augmented by an adaptive mechanism which identifies the scale factor and estimates the range (height) from optic flow, accelerometers data and pressure sensor measurements. the Adaptive Visual Odometer (AVO) generates estimates of the UAV velocity and position with respect to some initial rotorcraft location or some selected target. These visual estimates are then used in the guidance and flight control laws to guide the rotorcraft relative to the initial location or some moving/stationary target.

The proposed system is motivated by problems such as short-range navigation in GPS-denied environments for flight stabilization, accurate landing, target tracking, etc. To enable accurate and robust long-range navigation with the AVO, this latter can be combined with other terrain relative navigation techniques like landmarks recognition. An interesting approach could consist in performing landmarks matching and recognition in a moment-to-moment fashion (or periodically) to estimate the absolute position, and integrating the flight path between landmarks to estimate the relative position. Therefore, computation of distance flown is recommenced whenever a prominent landmark is encountered. Re-setting the AVO at each landmark facilitates accurate long-range navigation by preventing excessive accumulation of odometric errors. Indeed, some animals like bees seem to use landmark-based cues as well as visual path integration to navigate to a goal [12]. In this paper, we focus on the AVO for estimating the vehicle's velocity and position relative to some known location like the initial UAV location or a recognized landmark.

In the next section, the proposed visual navigation system is presented. Section III provides an overview of the aerial robotic platform, used for validating our system. Experimental results from autonomous flights of a quadrotor UAV are presented in Section IV.

II. VISUAL RELATIVE NAVIGATION SYSTEM

The proposed vision system determines the vehicle's relative velocity and 3D position with respect to the initial rotorcraft location or some target which may be stationary or moving. It relies on tracking features appearing in a "target template" initially chosen at the image center. With the computed template location (x_i, y_i) in the image frame, the relative distance (X_i, Y_i) between the rotorcraft and the ground objects appearing in the image template "i" is estimated after compensating the rotation effects using IMU data and recovering the range Z (or height) using an adaptive algorithm. The rotorcraft horizontal motion (X, Y) in the inertial frame is then estimated by accumulating or summing the relative distances (X_i, Y_i) for $i = 1...n$ as shown in Figure 2.

In this section, we describe the different components of our system which are: 1) image processing algorithm; 2) rotation effects compensation; 3) flight path integration; 4) range (height) sensing; and 5) velocity and position estimation.

A. Image processing for target template tracking

The main objective of this vision algorithm is to extract useful information from images about the UAV motion and its environment. The proposed approach relies on computing the image location and velocity of some target template by means of features tracking and optic flow computation.

In the beginning, an image area of 50×50 pixels, which can be considered as a "target template", is initially chosen at the image center. About 20 features are then selected automatically in that template using the Shi-Tomasi [13] algorithm. These features are then tracked in the successive images using the pyramidal Lucas-Kanade algorithm [14]. The outputs of this tracker are the features positions in the image frame. We have slightly modified that algorithm in order to provide also estimates about the optic flow at each feature location. The position (x_i, y_i) and velocity $(\dot{x}_i, \dot{y}_i)$ of the target template "i" is simply computed by taking the mean of the tracked features positions and velocities (or optic flow). For accurate and robust image template tracking, we have implemented simple routines that detect and handle features dispersion (features go out of the template) and erroneous feature correspondences which are mainly due to image noise and large attitude changes. For example, new features are selected in the same template when the variance of features positions exceeds sone threshold.

As the rotorcraft moves, older features leave the camera FOV and new features enter the FOV. Therefore, a new target template (or new set of features) is selected at the image center when the current template is about to go out of view.

B. Rotation effects compensation using IMU data

Image displacements occur with rotorcraft translation and orientation. Therefore, in order to sense aircraft translation which is essential for flight control, rotation effects must be eliminated from the measured image displacement and optic flow. This translation-rotation ambiguity is more significant in rotorcraft UAVs since the vehicle translation is a direct result of its attitude change. To overcome this problem and compensate the rotational components of optic flow and image displacement, onboard IMU data (Euler angles (θ, ϕ) and angular rate data $(\omega_x, \omega_y, \omega_z)$) are used.

$$\begin{cases} x_i^t = x_i - (-f \tan\theta) \\ y_i^t = y_i - (f \tan\phi) \end{cases} \quad (1)$$

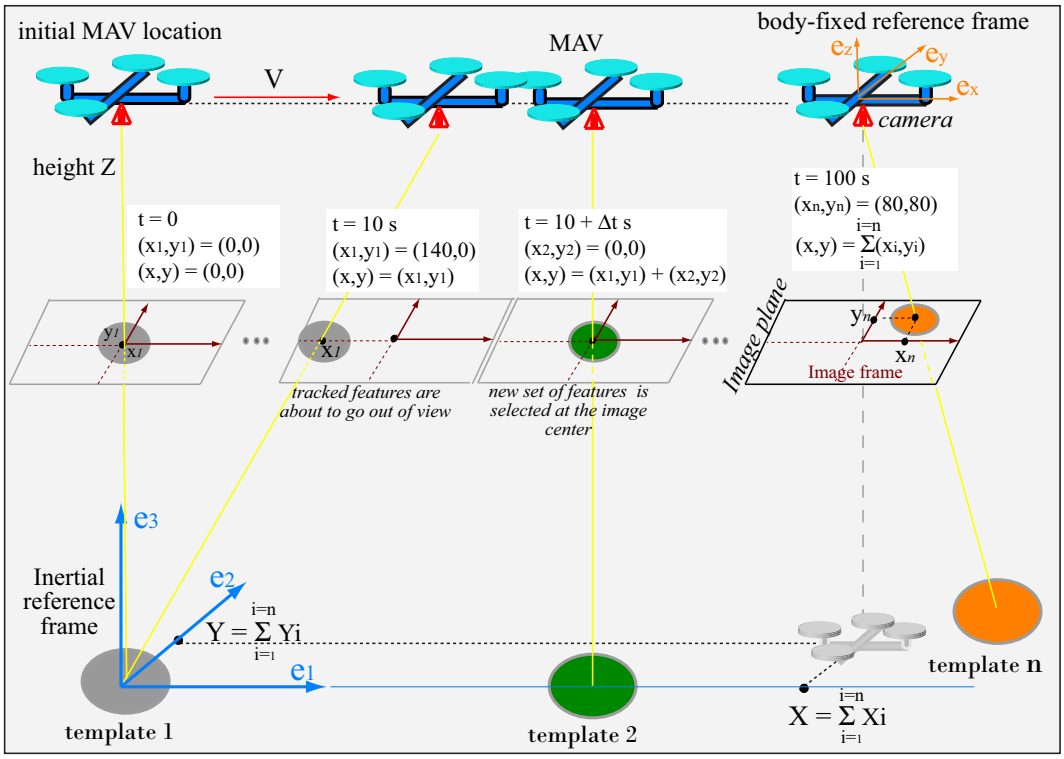

Fig. 2. Rotorcraft position estimation by visually tracking ground objects that appear in the camera field of view.

and

$$\begin{cases} \dot{x}_i^t = \dot{x}_i - (\frac{x_i y_i}{f}\omega_x - \frac{f^2+x_i^2}{f}\omega_y + y_i\omega_z) \\ \dot{y}_i^t = \dot{y}_i - (\frac{f^2+y_i^2}{f}\omega_x - \frac{x_i y_i}{f}\omega_y - x_i\omega_z) \end{cases} \quad (2)$$

where f is the camera focal length, (x_i^t, y_i^t) and $(\dot{x}_i^t, \dot{y}_i^t)$ are the translational components of the image displacement and optic flow caused by rotorcraft translation.

C. Flight path integration by image motion accumulation

Findings on insects navigation indicate that some insects like ants and honeybees posses a visually driven odometer that estimates distance flown by integrating the image motion [12]. In this research, we investigate the possibility of using a similar mechanism for mini rotorcraft navigation.

In order to provide a *pseudo*[1] position estimate relative to the initial UAV location, the total image displacement (x, y) is incremented when a template leaves the FOV and a new one is selected. Thus, the travelled flight distance or the total image displacement due to UAV translation can be computed as follows (see Figure 2):

$$\begin{cases} x^t = \sum_{i=1}^{i=n} x_i^t \\ y^t = \sum_{i=1}^{i=n} y_i^t \end{cases} \quad (3)$$

[1]We write pseudo position because it is expressed in the image frame in terms of image displacement [pixels].

with "n" is the number of the current template and (x_i^t, y_i^t) is the translational component of the last known position of the template "i" before leaving the camera FOV.

At this stage, we have visual information $(x^t, y^t, \dot{x}^t, \dot{y}^t)$ about the rotorcraft position and velocity which are expressed in terms of image displacement (pixels) and optic flow (pixels/s). The UAV position and velocity in the inertial frame can not be directly deduced because of the range ambiguity. Indeed, the translational image displacement depends on both aircraft translation and relative distance (range) to the perceived objects.

D. Range estimation by fusing optic flow and accelerometers measurements

The visual odometer presented in this paper requires an approximate measure of height above the ground in order to transform pixels into meters and recover the UAV position and velocity in the inertial frame.

Here, we show that under some conditions, it is possible to recover the range using only visual measurements from a single camera and linear accelerations data from IMU. Let us write the relation between the translational optic flow $(\dot{x}^t, \dot{y}^t)$ and the height Z:

$$\begin{cases} \dot{x}_i^t = f\frac{V_x}{Z} + x_i\frac{V_z}{Z} \\ \dot{y}_i^t = f\frac{V_y}{Z} + y_i\frac{V_z}{Z} \end{cases} \quad (4)$$

with (V_x, V_y, V_z) are the components of the rotorcraft velocity vector in the inertial frame and (x_i, y_i) is the image template position in the image frame where optic flow is computed.

As a first step, we propose a real-time identification algorithm that will estimate the range Z under the following assumptions:

1) The height changes are small ($Z \approx cst$ and $V_z \approx 0$) when applying the identifier.
2) The terrain or relief is smooth such that it can be decomposed into flat segments.

By differentiating equation (4) with respect to time and considering the above assumptions, we obtain:

$$\begin{cases} \dot{x}_i^t \backsimeq f \dfrac{a_x}{Z} \\ \dot{y}_i^t \backsimeq f \dfrac{a_y}{Z} \end{cases} \tag{5}$$

where (a_x, a_y) are the UAV linear accelerations expressed in the inertial frame which are obtained from the IMU.

Many types of on-line parameter estimation techniques can be applied to equation (5) in order to estimate Z using the derivatives of optic flow and linear accelerations. Our odometer uses the Recursive-Least-Squares (RLS) algorithm which presents many advantages for our application. For more robustness, we have used a robust variant of the RLS algorithm which includes a forgetting factor, dead zone and projection [15]. A detailed description of the identification process as well as stability analysis can be found in our previous paper [16].

***Remark** 1: The height estimation process suffers from the general well-known drawbacks of identification algorithms like noise and poor input-output signals (non-excited system). During real-time experiments, we have noticed performance degradation in height estimation by the RLS algorithm when the rotorcraft is hovering or flying at very low speeds. In this case, input and output signals are small compared to the noise level and do not contain sufficient information to estimate the height. As explained in [16] and [15], this is related to the persistent excitation (PE) property which is not satisfied in this case.*

This issue has been handled by switching off the adaptation process when the input and output signals are small (stationary or slow flights). In this case, height estimate is primary provided by the pressure sensor as a propagation of previous estimates using a kinematic Kalman filter. We would like to highlight that pressure sensor is lightweight (few grams), cheep (few dollars), and can be thus easily integrated into miniature air vehicles and combined with vision to improve height estimation and control.

E. Adaptive observer for position and velocity estimation

Once the height $\hat{Z}$ is identified, the aircraft horizontal position (X, Y) and velocity (V_x, V_y) can be recovered using the camera perspective projection model. Therefore, we can write:

$$\begin{cases} \hat{X} = \hat{Z} \dfrac{x^t}{f} \\ \hat{Y} = \hat{Z} \dfrac{y^t}{f} \end{cases} \text{ and } \begin{cases} \hat{V}_x = \hat{Z} \dfrac{\dot{x}^t}{f} \\ \hat{V}_y = \hat{Z} \dfrac{\dot{y}^t}{f} \end{cases} \tag{6}$$

***Remark** 2: It is important to note that (x^t, y^t) in (6) is the accumulated translational image displacement as shown in (3). Hence, the estimates $(\hat{X}, \hat{Y})$ in (6) correspond to the rotorcraft position in the inertial frame provided that the UAV flies at a constant height during path integration.*

For accurate position estimation even at varying height, it is better to estimate first the relative distances between the MAV and the tracked objects and then to accumulate these relative distances in order to provide an estimate of the MAV position in the inertial frame which is associated to the initial location, Figure 2. This is mathematically equivalent to:

$$\begin{cases} \hat{X} = \sum_{i=1}^{i=n} X_i = \sum_{i=1}^{i=n} \hat{Z}_i \dfrac{x_i^t}{f} \\ \hat{Y} = \sum_{i=1}^{i=n} Y_i = \sum_{i=1}^{i=n} \hat{Z}_i \dfrac{y_i^t}{f} \end{cases} \tag{7}$$

The last step of the visual odometer consists in fusing the visual estimates $(\hat{X}, \hat{Y}, \hat{Z}, \hat{V}_x, \hat{V}_y)$ and INS data (a_x, a_y, a_z) in order to improve the odometer accuracy and robustness, reduce the noise and estimate the vertical velocity V_z. The data fusion is performed using a linear Kalman filter with choosing (X, Y, Z, V_x, V_y, V_z) as a state vector, $(\hat{X}, \hat{Y}, \hat{Z}, \hat{V}_x, \hat{V}_y)$ as a measurement vector and (a_x, a_y, a_z) as an input vector. The implementation of such Kalman filter is straightforward and thus further details are omitted here.

III. AERIAL PLATFORM DESCRIPTION AND SOFTWARE IMPLEMENTATION

A. Quadrotor-based aerial platform

Our platform is based on a miniature (53 cm) four-rotor helicopter, called *X-3D-BL*. To demonstrate autonomous flight, we have fitted the helicopter with an embedded autopilot that we have developed and presented in our previous paper [17]. The hardware components that make up the basic flight avionics of our platform include a small micro-controller from *Gumstix Inc.* and the MNAV100CA sensor from *Crossbow Inc.* which includes a digital IMU, a GPS receiver and a pressure sensor in one compact sensor. Our imaging system includes a small analog camera from *RangeVideo* and a 1.3 GHz video transmitter.

The total weight of the aerial vehicle is about 650 grams including the air vehicle, battery, Flight Control Computer (FCC), sensors and vision system.

B. Real-time software

In order to demonstrate vision-based autonomous flight, we have implemented the navigation and control algorithms on the onboard FCC including some parts of the adaptive visual odometer. We have also developed a real-time software for the Ground Control Station (GCS) which implements the image processing algorithm (see subsection II-A) and other routines for flight data displaying. The visual measurements are provided at 10 Hz and sent to the onboard FCC through WiFi communication using UDP protocol.

The real-time embedded software is implemented as a process within Linux OS, and it is composed of five tasks or threads, that are called and scheduled separately, Figure 3. The adaptive visual odometer provides position, velocity

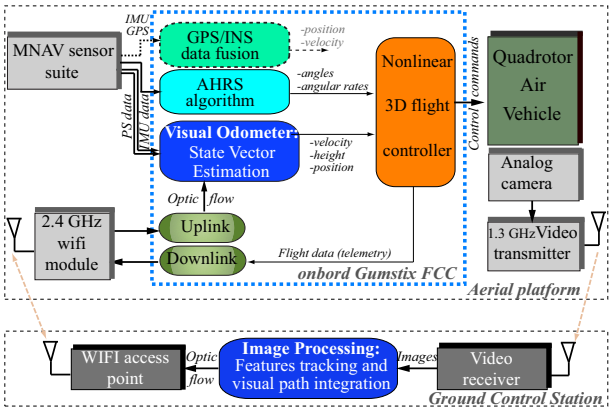

Fig. 3. Real-time architecture of the vision-based autopilot.

and height estimates at an updating rate of 10 Hz, which are then used by a nonlinear controller for achieving autonomous vision-based flight. Details about the design and implementation of the flight controller can be found in [17].

IV. EXPERIMENTS

The performance of the vision-based navigation system is demonstrated in real flights using the quadrotor MAV described in the previous Section. Here, we present experimental results from three test flights under autonomous control.

A. Automatic take-off, accurate hovering and precise auto-landing on some arbitrary target

As described in Section II, the target template is initially chosen at the image center. However, the developed GCS and embedded software allow to choose this target template at any image location by just selecting the desired area/object on the image displayed at the GCS. This flight test consists in exploiting this useful characteristic to achieve an accurate hovering above some designated ground target and to perform a precise auto-landing on it.

The rotorcraft was put on a small box of about 50cm x 70cm which is used as a target, Figure 1. The take-off procedure is launched from the GCS and the target is selected when it appeared in the camera FOV (about 1m height during take-off). When the MAV reached the desired height of 10 m, it performed an accurate hovering by tracking the target and keeping it at the image center. Finally, the auto-landing procedure is activated and the MAV executed descent flight while controlling its horizontal position to keep the target at the image center.

Figure 4 shows the obtained MAV trajectories (position and height). The relative horizontal position between the MAV and the target was regulated to zero with about $\pm 0.5m$ maximum error. The height is also estimated and controlled accurately yielding to automatic take-off and auto-landing. The MAV achieved successfully the assigned task by relying on the visual estimates, as it can be seen in the associated video clip:

http://jp.youtube.com/watch?v=rbmsivw5luk&feature=channel_page

B. Vision-based tracking of a moving ground target

Here, we explore the possibility of our vision-control system to track a moving ground target. For this experiment, we have used a small cart (see Figure 6) as a target and placed it at about 20 m from the GCS.

Figure 5 shows that the target is accurately tracked even when it is moving. The GPS ground-track on the first graph shows that the MAV flied about 20m (which corresponds also to the target movement) from the initial location while controlling the relative position MAV-target to zero with $\pm 1m$ maximum error during tracking. Video clip of this flight

(a) (b)

Fig. 6. (a) onboard camera image showing visual tracking of a moving target; (b) the quadrotor during vision-based tracking of a moving target.

test is available at:

http://jp.youtube.com/watch?v=6obHavVvJyk&feature=channel_page

C. GPS-based waypoint navigation and comparison with the visual estimates

In this test, we have performed autonomous waypoint navigation using GPS data for motion control. The objective of this test is to evaluate the performance of the adaptive visual odomter for estimating the vehicle's position during translational flight. The obtained results from GPS and vision system are shown in Figure 7.

One can see that the reference trajectories are tracked and the mission is accomplished. It is also important to note that during this translational flight, the odomter was able to estimate the MAV position or the travelled flight distance despite the poor texture of the terrain (play-ground). The errors between GPS measurements and visual estimates may be attributed to inaccuracies in path integration and identification errors during height estimation.

V. CONCLUSION

In this paper, a vision-based navigation system for micro air vehicles is presented. It is based on features tracking and path integration using images from an onboard camera and inertial measurements from a low-cost IMU. The vision algorithm has been augmented by an adaptive observer that fuses visual measurements with accelerations and pressure sensor data in order to estimate the vehicle's height, velocity and position relative to an initial location or some selected target. The experimental results from autonomous flights show that the adaptive visual odometer is able to estimate the vehicle's motion in unknown environments and to guide a rotorcraft MAV to achieve various navigation tasks such as hovering, precise auto-landing and moving target tracking.

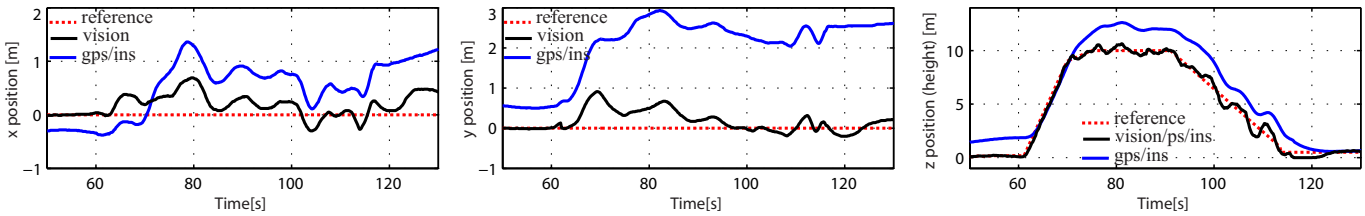

Fig. 4. Accurate hovering and precise auto-landing on some designated ground target. Visual estimates are more accurate than GPS measurements. The MAV landed at about 25 cm from the target, but it can be seen from the video that the MAV was exactly on the target at 30 cm height and then landed just near the target. This is due to very large image displacements when the MAV is at few centimeters from the target or ground. One approach to solve this problem could consist in deactivating the visual odometer and decrementing the thrust when the aircraft height is under some threshold (50cm for example).

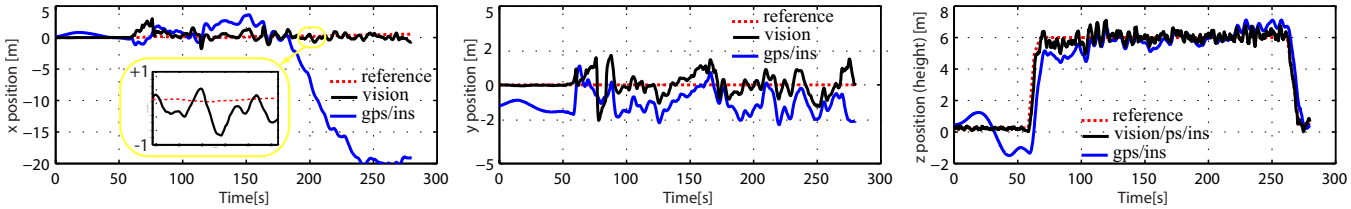

Fig. 5. Application of the vision-based autopilot for tracking a moving target. First, the MAV performed automatic take-off from the target and hovered above the target (6m height) for nearly 100 s. Then, the target is continuously moved towards the GCS by pulling some wire attached to the target. The control objective is thus, to keep the moving target at the image center by controlling the relative position between the MAV and the target to zero.

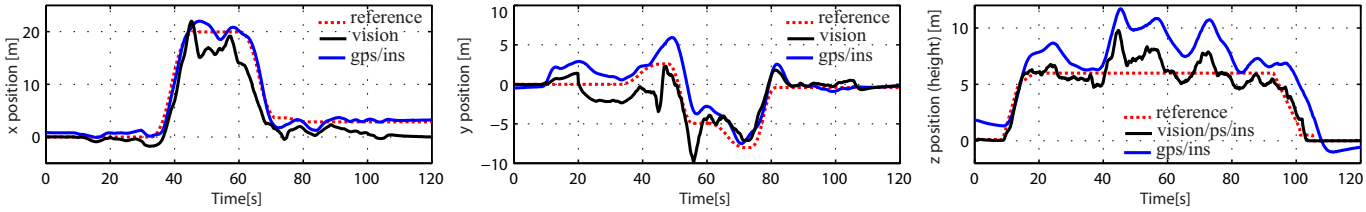

Fig. 7. GPS waypoint navigation and comparison with the visual odometer estimates.

REFERENCES

[1] S. Scherer, S.Singh, L. Chamberlain, and M. Elgersma, "Flying fast and low among obstacles: Methodology and experiments," *International Journal of Robotics Research*, vol. 27, no. 5, pp. 549–574, May 2008.

[2] R. He, S. Prentice, and N. Roy, "Planning in information space for a quadrotor helicopter in a GPS-denied environment," in *Proceedings of the IEEE International Conference on Robotics and Automation*, California, USA, May 2008, pp. 1814–1820.

[3] S. Grzonka, G. Grisetti, and W. Burgard, "Towards a navigation system for autonomous indoor flying," in *Proceedings of the IEEE International Conference on Robotics and Automation*, Kobe, Japan, May 2009, pp. 2878–2883.

[4] J. Kima and S. Sukkarieh, "Real-time implementation of airborne inertial-slam," *Robotics and Autonomous Systems*, vol. 55, pp. 62–71, 2007.

[5] F. Caballero, L. Merino, J. Ferruz, and A. Ollero, "Vision-based odometry and slam for medium and high altitude flying uavs," *Journal of Intelligent Robotic Systems*, vol. 54, pp. 137–161, 2009.

[6] O. Amidi, T. Kanade, and K. Fujita, "A visual odometer for autonomous helicopter fight," *Robotics and Autonomous Systems*, vol. 28, no. 2-3, pp. 185–193, 1999.

[7] A. Johnson, J. Montgomery, and L. Matthies, "Vision guided landing of an autonomous helicopter in hazardous terrain," in *Proceedings of the 2005 IEEE International Conference on Robotics and Automation (ICRA)*, Barcelona, Spain, April 2005, pp. 4470–4475.

[8] T. Kanade, O. Amidi, and Q. Ke, "Real-time and 3d vision for autonomous small and micro air vehicles," in *Proc. of the 43rd IEEE Conference on Decision and Control*, Atlantis, Paradise Island, Bahamas, December 2004, pp. 1655–1662.

[9] F. Kendoul, I. Fantoni, and K. Nonami, "Optic flow-based vision system for autonomous 3D localization and control of small aerial vehicles," *Robotics and Autonomous Systems (Elsevier)*, vol. 57, pp. 591–602, 2009.

[10] S. Saripalli, J. Montgomery, and G. Sukhatme, "Visually-guided landing of an unmanned aerial vehicle," *IEEE Transactions on Robotics and Automation*, vol. 19, no. 3, pp. 371–381, 2003.

[11] E. N. Johnson, A. J. Calise, Y. Watanabe, J. Ha, and J. C. Neidhoefer, "Real-time vision-based relative aircraft navigation," *Journal of Aerospace Computing, Informatiom, and Communication*, vol. 4, pp. 707–738, April 2007.

[12] M. V. Srinivasan, S. Zhang, and N. Bidwell, "Visually mediated odometry in honeybees," *The Journal of Experimental Biology*, vol. 200, pp. 2513–2522, 1997.

[13] J. Shi and C. Tomasi, "Good features to track," in *Proceedings of the IEEE Conference on Computer Vision and Pattern Recognition*, ser. Seattle, WA, USA, 1994, pp. 593–600.

[14] B. Lucas and T. Kanade, "An iterative image registration technique with an application to stereo vision," in *Proc. DARPA IU Workshop*, 1981, pp. 121–130.

[15] P. Ioannou and J. Sun, *Robust Adaptive Control*. Prentice Hall Inc, 1996.

[16] F. Kendoul, I. Fantoni, and R. Lozano, "Adaptive vision-based controller for small rotorcraft uavs control and guidance," in *Proceedings of the 17th IFAC World Congress*, Seoul, Korea, July 6-11 2008, pp. 797–802.

[17] F. Kendoul, Y. Zhenyu, and K. Nonami, "Embedded autopilot for accurate waypoint navigation and trajectory tracking: Application to miniature rotorcraft uavs," in *Proceedings of the IEEE International Conference on Robotics and Automation*, Kobe, Japan, May 2009, pp. 2884–2890.